Corrosion Science 79 (2014) 29–33

Contents lists available at ScienceDirect

Corrosion Science

journal homepage: www.elsevier.com/locate/corsci

# The effect of grain boundaries on high temperature oxidation of new $\gamma'$-strengthened Co–Al–W–B superalloys

L. Klein, B. von Bartenwerffer, M.S. Killian, P. Schmuki, S. Virtanen *

*Department of Materials Science and Engineering, Institute for Surface Science and Corrosion (LKO), University of Erlangen-Nürnberg, Martensstr. 7, 91058 Erlangen, Germany*

ARTICLE INFO

*Article history:*
Received 3 July 2013
Accepted 16 October 2013
Available online 23 October 2013

*Keywords:*
A. Superalloys
A. Cobalt
B. SIMS
C. Oxidation

ABSTRACT

Isothermal oxidation in air was carried out on a $\gamma'$-strengthened single crystalline Co–Al–W–B superalloy at 800, 900, and 1000 °C. The absence of grain boundaries leads to inferior oxidation properties at 800 and 900 °C, and improved properties at 1000 °C, compared to a polycrystalline alloy of the same composition. At lower temperatures, grain boundary diffusion is dominant and assumed to be the reason for enhanced B-accumulation in the inner oxide layer and enhanced formation of the protective inner $Al_2O_3$ layer. However, at 1000 °C superior oxidation resistance of the single crystalline superalloy can be observed.

## 1. Introduction

In the course of the last decades, $\gamma'$-strengthened Ni-base superalloys became the most common used material for high temperature applications, such as discs and blades in aircraft engines and industrial steam turbines. Here, a combination of excellent mechanical properties (creep strength, ductility) and good oxidation resistance at high temperatures is required [1]. For this reason, conventional Co-base superalloys, which exhibit superior corrosion resistance but inferior mechanical properties compared to common Ni-base superalloys, are used mainly in corrosive environments or mechanically lower loaded regions of turbines [2,3]. High temperature strength of Ni-base superalloys results from a stable ternary $Ni_3Al$ compound with an $L1_2$ structure, which precipitates as a cuboidal so called $\gamma'$-phase in the fcc $\gamma$-Ni solid solution [2,4]. Since 2006, a novel $\gamma'$-strengthened Co-base superalloy is under investigation exhibiting high temperature strength values in the range of Ni-base superalloys [5]. Strengthening can be achieved by a $Co_3(Al,W)$ phase in the $\gamma$-Co matrix, similar to the $Ni_3Al$ phase in Ni-base superalloys [5]. Furthermore, the addition of Ta or Ti results in $\gamma'$-solvus temperatures higher than those of commercial Ni-base superalloys, such as Waspaloy [5]. It was also reported by Sato et al. that the melting temperatures of polycrystalline Co–Al–W based alloys is 50–100 K higher compared to Ni-based alloys [5,6] which would lead to increased process temperatures of future turbine generations. Recent publications [7,8] confirm that previous improvements in mechanical properties of polycrystalline alloys due to B addition [2,9,10] can also be achieved for novel Co-base superalloys by means of grain boundary strengthening. Nevertheless, relatively poor oxidation resistance is still a major drawback of this new alloy system and has to be improved significantly, since lifetime of high temperature materials is decreased by oxidation as it impairs the mechanical properties.

Compared to Ni-base superalloys [11–15], only very little research has been done so far concerning oxidation properties of $\gamma'$-strengthened Co-base superalloys [16]. For this reason, Klein et al. [17–20] recently investigated the long term oxidation properties and mechanisms of polycrystalline Co–Al–W based alloys between 800 and 1000 °C in air and revealed the effects of different alloying elements, such as B, Cr, Ni and Si. The most interesting effect is the significant improvement in oxidation resistance and oxide layer adhesion due to sufficient amounts of B in the alloy (0.12 at.%). Results show that B strongly benefits inner $Al_2O_3$ formation with increasing oxidation time, and presumably W-borides in the inner oxide layer can be attributed to improved scale adhesion. In contrast to polycrystalline $\gamma'$-strengthened Co-base superalloys, oxidation properties of single crystalline Co-base alloy variants have not been investigated and compared to polycrystalline alloys so far. It is assumed that the absence of grain boundaries in Co–Al–W based superalloys significantly influences the oxidation performance at high temperatures due to changes in the diffusion mode (grain boundary diffusion versus volume diffusion). In order to clarify this, high temperature oxidation properties of novel $\gamma'$-strengthened polycrystalline and single crystalline Co–Al–W–B superalloys were explored in the present study between 800 and

---

* Corresponding author. Tel.: +49 9131 8527577; fax: +49 9131 8527582.
*E-mail addresses:* leonhard.klein@ww.uni-erlangen.de (L. Klein), bernd@vonbartenwerffer.de (B. von Bartenwerffer), manuela.killian@ww.uni-erlangen.de (M.S. Killian), schmuki@ww.uni-erlangen.de (P. Schmuki), virtanen@ww.uni-erlangen.de (S. Virtanen).

0010-938X/$ - see front matter © 2013 Elsevier Ltd. All rights reserved.
http://dx.doi.org/10.1016/j.corsci.2013.10.022

1000 °C in air. In addition to thermogravimetric analysis, characterisation of the oxide layers, the alloy composition and the alloy microstructure was carried out by means of scanning electron microscopy (SEM) and energy dispersive X-ray spectroscopy (EDX). Furthermore, the influence of high temperature oxidation on the distribution of B within the oxide layer was of interest. For this, time-of-flight secondary ion mass spectrometry (ToF-SIMS) analysis was performed.

## 2. Experimental

The experimental single crystalline superalloy was cast by the Institute of Metals Science and Technology (WTM, University of Erlangen-Nürnberg, Germany) in a Bridgman vacuum investment casting facility as a cylindrical bar with a diameter of approximately 12 mm. The crystal orientation deviates from the [001] direction by approximately 20°. The mean composition of the investigated Co–9Al–9W–0.12B alloy (in the following abbreviated as “SX 0.12B”) was determined by energy dispersive X-ray spectroscopy (EDX, Oxford Instruments Inc.) as 81.1Co–9.2Al–9.8W (in at.%; standard deviation of measured values smaller than 0.15 at.%). Due to insufficient melting of W during the casting process, certain deviations from the nominal composition may occur. In addition, the B-content of the alloy (0.12 at.%) was confirmed by glow discharge optical emission spectroscopy (GDOES, RF GD Profiler, HORIBA Jobin Yvon GmbH) at Neue Materialien Fürth (NMF), since B is a light element and hard to detect by EDX. Furthermore, the detection limit of EDX is too high (approximately 0.1 at.%) in order to measure such small B-contents.

The as-cast alloy was homogenised at 1300 °C for 12 h in protective Ar-atmosphere and aged for 200 h at 900 °C in air, in order to obtain the desired $\gamma/\gamma'$-microstructure. The generated oxide layer on the sample surface was completely removed subsequent to aging of the alloy in air. After cutting disc-shaped specimens from the cylindrical bar and drilling a 2 mm pin hole in each sample (for suspension in the high temperature furnace), wet grinding and polishing was performed using SiC grinding paper (up to grit 1200) and different diamond suspensions (up to a grain size of 1 μm), respectively. The size of the ready-prepared oxidation samples amounted to 11.0 mm in diameter and 2.0 mm in height.

Long-term isothermal oxidation experiments were conducted for 500 h at 800, 900, and 1000 °C in a vertical tube furnace under atmospheric conditions. The specimens were attached to a microbalance (accuracy ±0.01 mg) by means of a heat resistant freely suspended platinum or NiCr wire and introduced into the furnace after reaching the set temperature. Mass change (in mg/cm$^2$) was determined simultaneously with increasing oxidation time by thermogravimetric analysis (TGA). Reproducibility of the oxidation curves was assured by performing three different measurements at each temperature. Therefore, in the results section of the present work, representative curves are given. After finishing the TGA, the oxidised specimens were immediately removed from the furnace and cooled off at room temperature.

The morphology of the generated oxide layers and the $\gamma/\gamma'$-microstructure were investigated by SEM (Jeol JSM 6400 and FE-SEM Hitachi S-4800) of prepared cross-sections, using the BSE (backscattered electron) mode for elemental contrast imaging. Improved quality of the $\gamma/\gamma'$-microstructural image was achieved by etching the sample with 100 ml of distilled water, 50 ml of 40% HCl, 5 ml of 70% HNO$_3$, and 0.15 ml of Dr. Vogel’s Spar etchant consisting of 30% 1-methoxy-2-propanol and 2.5% thiocarbamide. In order to calculate mean oxide layer thicknesses (and the corresponding standard deviations), at least 15 measurements were performed using several representative SEM micrographs and the image processing programme “ImageJ”.

Time-of-flight secondary ion mass spectrometry (ToF-SIMS, ION-TOF GmbH Münster, TOF.SIMS 5 spectrometer) allowed for determination of the B-distribution within the oxide layer by investigating cross-sections of the oxidised alloy. The sample was irradiated with a pulsed 25 keV Bi$^+$ liquid–metal ion beam. Signals were identified according to their accurate mass and isotopic pattern in the high mass resolution mode and B-mappings were recorded in high lateral (and low mass) resolution mode. A lateral resolution of 200–300 nm and a sampling depth of approximately 10–20 Å was achieved with this setting. Images were recorded in positive (and for completion also in negative) polarity and care was taken not to exceed the static limit of 10$^{13}$ ions cm$^{-2}$. The brightest pixel in the chemical map corresponds to the largest number of counts.

In order to highlight the influence of grain boundaries on oxidation properties, the results of the SX 0.12B alloy were compared to a polycrystalline alloy (in the following abbreviated as “0.12B”) of the mean composition 81.8Co–8.8Al–9.3W–0.12B (in at.%), which was oxidised for 500 h at 800, 900, and 1000 °C in air. Some results of the investigated 0.12B alloy were previously published in Corrosion Science [17,18].

## 3. Results

Due to the specific heat treatment process consisting of homogenisation and aging, the investigated SX 0.12B superalloy establishes the desired $\gamma/\gamma'$ microstructure. In Fig. 1, a representative SEM image of the etched metal surface is given. The cuboidal $\gamma'$-phase shows a sufficiently high volume fraction and is homogeneously distributed in the $\gamma$-matrix. A direct comparison of the SX 0.12B alloy (see Fig. 1) with a previously investigated polycrystalline 0.12B alloy [17,20] of comparable composition reveals similar $\gamma/\gamma'$ microstructures.

In order to investigate the oxidation behaviour at high temperatures and to highlight the influence of grain boundaries, long-term thermogravimetric experiments were carried out on polycrystalline and SX 0.12B superalloys at 800, 900, and 1000 °C in air (see representative curves in Fig. 2). The results of the polycrystalline 0.12B alloy at 800 and 900 °C [17] serve as a comparison to the currently investigated SX 0.12B alloy. In general, after short exposure times a transient oxidation period can be observed for both alloys at each temperature, characterised by heavy mass gain. However, mass gain strongly decelerates in the course of high temperature oxidation. At 800 °C, the polycrystalline alloy shows highly improved oxidation resistance with respect to the SX alloy of the same composition. After approximately 100 h of oxidation, no further oxidation can be measured in case of the polycrystalline alloy whereas the SX 0.12B alloy shows continuous oxidation during the entire long-term measurement. Hence, formed oxide layers on the polycrystalline alloy are

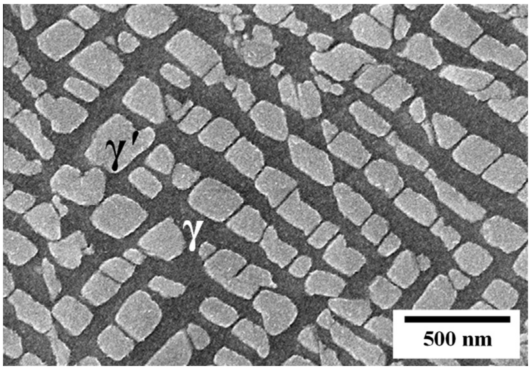

**Fig. 1.** $\gamma/\gamma'$ microstructure of the etched SX 0.12B alloy.